A new deterministic CA model for traffic flow with multiple states

Katsuhiro Nishinari[a] and Daisuke Takahashi[b]

[a] Department of Mechanical Engineering, Faculty of Engineering, Yamagata University, Yonezawa, Yamagata 992, JAPAN

knishi@dips.dgw.yz.yamagata-u.ac.jp

[b] Department of Mathematical Sciences, Waseda University, Ohkubo 3-4-1, Shinjuku-ku, Tokyo 169, JAPAN

daisuke@mse.waseda.ac.jp

Abstract

In this paper, an ultra-discrete version of the Burgers equation, which includes the rule-184 CA model, is extended to treat a higher velocity. The extended model has multiple states at the transition region of car density from free to congested phase in the fundamental diagram. State of free phase at high density is unstable to perturbation, and its stability is discussed in detail.

1 Introduction

Traffic flow is a complex discrete system and its analysis is one of main themes in complex system theory. It shows interesting collective behaviors, such as pattern formation, phase transition and scale invariant fluctuations. The system has been studied by many different approaches, which can be broadly divided into two categories; macroscopic and microscopic ones. Macroscopic approaches are based on hydrodynamical equations[1][2]. In these approaches, we need an empirical steady flow-density relation from some observed data in order to analyze time evolution of traffic flow. Flow versus density diagram of steady states is called fundamental diagram.

In order to explain the diagram itself, we use microscopic approaches instead of macroscopic ones. Microscopic approaches are called car-following theory, because a behavior of each vehicle is modeled in relation to a vehicle ahead. First, Newell introduced a preferred velocity function and obtained a differential delay equation[3]. Recently, an optimal velocity model is proposed by Bando *et al*[4], and they have introduced a semi-empirical function of desirable velocity depending on headway distance. They also obtained a fundamental diagram, in which they can successfully shows an existence of discontinuity at a critical density of transition from free flow to congested one[5]. Let us see here an example of fundamental diagram of observed data taken by the Japan Highway Public Corporation[6](Fig.1). We find a discontinuity at the occupancy $\sim 25\%$, and there seems to exist multiple states around the critical occupancy. Many other real diagrams show this type of graphs and the flow-density curve shows a shape of "inverse λ"[6]. This discontinuity has been explained by many researchers. Edie introduced a discontinuity by hand by using the Greenberg's model[7]. Navin and Hall proposed three-dimensional space of data, i.e., relation among flow, velocity and density, and explained the discontinuity by using the catastrophe theory[8].

Newer development of traffic flow theory is a cellular automaton (CA) model. CA

model is quite simple and has flexibility, and suitable for computer simulations of discrete phenomena[9]. Nagel and Schreckenberg(NS) proposed a stochastic traffic CA for the description of single-lane highway traffic. The NS model is able to reproduce the spontaneous formation of jams by introducing braking probability in its evolutional rule[10][11]. Fukui and Ishibashi introduced a deterministic CA model by using the rule–184 CA[12]. Fukś and Boccara also proposed deterministic CA models by extending the rule–184 CA[13]. The rule–184 CA is widely used as a prototype of deterministic model of traffic flow. The fundamental diagram of the NS model does not show discontinuity at a critical density[14]. Those of deterministic models that use the rule–184 CA also does not show such discontinuity and multiple states, even though they show sharp phase transition[13]. A CA model which shows the discontinuity is obtained first in [15]. In their model, a deterministic rule, so-called "slow-to-start" rule, is introduced and multiple states in the fundamental diagram are demonstrated. In [16] and [17], stochastic slow-to-start rule is introduced by considering that standing cars can be accelerated with lower probability than moving cars. Their models are generalizations of the NS model, and the existence of metastable states is shown in a density region close to the maximum flow.

Recently an ultra discrete version of the Burgers equation, that is, Burgers cellular automaton (BCA) has been proposed and used as a particle hopping model[18]. BCA is proved to contain the rule–184 CA as a special case, thus it is considered as a generalization of the rule–184 CA. In this paper, we extend BCA to treat a higher velocity, and we have found that our new deterministic CA model shows multiple states at a transition region in the fundamental diagram. Our model is fully deterministic and suitable to study detailed properties of discontinuity and multiple states in the diagram.

This paper is organized as follows. BCA is introduced as a traffic flow model and its properties and problems are discussed in Sec. 2. BCA is extended to treat a higher velocity and a fundamental diagram is analyzed in Sec. 3. In Sec. 4, unstable free flow is studied in detail and concluding discussions are given in Sec. 5.

2 BCA as a traffic flow model

2.1 A new CA model of traffic flow

BCA is given by[18]

$$U_j^{t+1} = U_j^t + \min(M, U_{j-1}^t, L - U_j^t) - \min(M, U_j^t, L - U_{j+1}^t). \tag{1}$$

It has been shown in [18] that (1) is related to the Burgers equation $v_t = 2vv_x + v_{xx}$ through the transformation $U_j^t = L/2 + \varepsilon \Delta x v(j\Delta x, t\Delta t)$, where Δx and Δt are lattice intervals in x and t respectively and ε is a parameter used in the ultradiscrete formula[19]. There are two parameters L and M in BCA. In our previous paper, we have shown following properties of this equation: assuming that $M > 0$, $L > 0$ and $0 \leq U_j^t \leq L$ for any site j at a certain time t, then, $0 \leq U_j^{t+1} \leq L$ holds for any j. Thus (1) is equivalent to a CA with a value set $\{0, 1, \cdots, L\}$ under the above conditions. Moreover, if we put a restriction $L \leq M$ and $L = 1$ on BCA, then BCA is equivalent to the rule–184 CA, which is used as a prototype of traffic flow models[12].

Then it is natural to consider (1) with general L and M as a traffic model. The road is expressed by a discrete space sites indexed by a site number j. We assume that the capacity of each site is L cars. U_j^t denotes the number of cars at site j and time t, which is an integer from 0 to L. Cars at site j and time t stay at site j or move to site $j+1$ at the next time $t+1$. The maximum number of movable cars is M. Under this restriction, they move to fill vacant spaces at site $j+1$. The second and the last term of the right hand side of (1) represents the number of cars that comes from the site $j-1$ and moves to the next site $j+1$, respectively. It is apparent that the total number of cars is preserved under the rule.

The physical meaning of this model may be interpreted as following two ways: first, the road is L-lane freeway in a coarse sense, and effect of lane changes of cars is not considered explicitly. Second, we consider single-lane freeway and U_j^t/L represents probability of

existing of a car at site j and time t. If we choose large L, U_j^t/L can take a fine value from 0 to 1. In the latter case, the number U_j^t itself no longer represents real number of cars at site j.

We define ρ by an average density of cars per site given by

$$\rho \equiv \frac{1}{KL}\sum_{j=1}^{K} U_j^t, \tag{2}$$

where we consider a periodic boundary condition to the road and K is a period in site number. Throughout this paper we assume that the road is periodic, or a circuit. Since the total number of cars is preserved, the density ρ is constant during the course of time. In order to describe the fundamental diagram, we define an average flow of cars by

$$q^t \equiv \frac{1}{KL}\sum_{j=1}^{K} \min(M, U_j^t, L - U_{j+1}^t). \tag{3}$$

By using (3) and (2), the fundamental diagram is shown in Fig.2 in the case $L \leq 2M$. The diagram shows steady-state, long time averages over the entire system starting from random initial conditions. The flow q^t becomes constant at large enough t. In a region of $\rho < 1/2$, all dots are exactly on a line $q = \rho$, and on a line $q = 1 - \rho$ in a region of $\rho > 1/2$ from any initial data. These facts have been proved by using an ultradiscrete diffusion equation[18]. There is a sharp transition point $\rho = 1/2$ which separates free laminar flow and congested flow. The fundamental diagram in Fig.2 is unique for any L and M ($L \leq 2M$), especially it is the same as that of the rule–184 CA ($L = 1$).

In the case $L > 2M$, the shape is trapezoidal(Fig.3). The steady flow of the region of the density $M/L \leq \rho \leq (L-M)/L$ has the constant value M/L. This result has been also proved in [18] relating the particle model. It should be noted that the shape of trapezoid is similar to that of Yukawa *et al*[20], who introduced a blockage site artificially in the rule–184 CA for taking the bottleneck of flow into account. The blockage site has some transmission probability in their model. Our model, however, is fully deterministic and contains a parameter M beforehand as a role of the flow limiter.

2.2 Properties and problems of BCA as a traffic model

In this subsection, we restrict ourselves to the case $L \leq 2M$ and $L = 2$ for simplicity and investigate detailed properties of BCA. We have seen above that the rule–184 CA and BCA show the same fundamental diagram. However, we should point out an important fact of BCA that multiple states are degenerated in the diagram. First, it is easily shown that BCA with $L = 2$ contains the rule–240, 184, 170 CA's[9] as a special case. In the case $U_j^t \in \{0, 1\}$ for all j, from (1) the truth value table of BCA is expressed symbolically by

$$\frac{U_{j-1}^t U_j^t U_{j+1}^t}{U_j^{t+1}} = \frac{000}{0}, \frac{001}{0}, \frac{010}{0}, \frac{011}{0}, \frac{100}{1}, \frac{101}{1}, \frac{110}{1}, \frac{111}{1},$$

then we see that $U_j^t \in \{0, 1\}$ for all t. This is nothing but the rule–240, and all patterns of "0" and "1" shift to the right. Next in the case $U_j^t \in \{0, 2\}$ we obtain

$$\frac{U_{j-1}^t U_j^t U_{j+1}^t}{U_j^{t+1}} = \frac{000}{0}, \frac{002}{0}, \frac{020}{0}, \frac{022}{2}, \frac{200}{2}, \frac{202}{2}, \frac{220}{0}, \frac{222}{2}.$$

This is the rule–184 of a value set $\{0, 2\}$. In the case $U_j^t \in \{1, 2\}$ we obtain

$$\frac{U_{j-1}^n U_j^n U_{j+1}^n}{U_j^{n+1}} = \frac{111}{1}, \frac{112}{2}, \frac{121}{1}, \frac{122}{2}, \frac{211}{1}, \frac{212}{2}, \frac{221}{1}, \frac{222}{2}.$$

This is the rule–170, and all patterns of "1" and "2" shift to the left.

Thus in the rule–240 CA, all cars expressed by the number "1" move right by one site in unit time in the background of 0's. All states constructed only from 0's and 1's are always less than 1/2 density and therefore plotted on line $O - A$ in Fig.2. Similarly, in the the rule–170 CA, the number "2", which stands for a full-packed site, propagates left in the background of 1's. The density of this case is always greater than 1/2 and it is apparent that all states are plotted on the line $A - B$. Steady states containing only "2" and "0" are spread on the 'hat' $O - A - B$, which is proved in [18]. Therefore the line $O - A$ contains at least two kinds of steady states, i.e., those of the rule–240 and rule–184. The line $A - B$ also contains steady states of the rule–170 and rule–184. Therefore it is

found that steady states that governed by different rules have the same traffic flow and car density in the BCA model. We call this situation as 'degenerated' in this paper. This is a crucial difference between BCA with $L \geq 2$ and BCA with $L = 1$(rule–184 CA). This fact plays an important role in the following sections.

BCA is, however, too simple to analyze the complexity of a congested flow. From Fig.1 mentioned in Sec. 1, the real flow does not show continuous transition from free to congested flow, but there is a discontinuity around the critical density, or flow q has multiple values at the same density ρ in the transition region. Although the fundamental diagram of Fig.2 shows the phase separation of free moving region and congested region, BCA is too simple to capture the nature of the transition from free to congested flow.

3 Extended BCA model

In the previous section, we see that multiple states are degenerated in the same value of ρ in BCA. We show in the followings that the degenerated states give remarkable changes to the fundamental diagram when we introduce higher velocity of cars. About the rule–184 CA model, the extension to higher velocities has been done by Fukui and Ishibashi[12], and they show that the critical density in the fundamental diagram becomes lower in the higher velocities. However, the fundamental diagrams in their model does not show discontinuity at the critical density.

Let us define the velocity V as maximum number of sites by which the car can advance in unit time. BCA is the case $V = 1$. We extend BCA to $V = 2$ in the following, and let us call this model 'extended BCA(EBCA)' in this paper. Following Ref.[12], we assume that a car can advance by two sites per time if the successive two sites are not fully occupied. The rule for shifting cars per time is given as follows: First, we consider that cars moving two sites have priority to those moving one site. Then the number of cars at site j that can move two sites forward is given by $a_j^t \equiv \min(U_j^t, L - U_{j+1}^t, L - U_{j+2}^t)$, where $L - U_{j+1}^t$ and $L - U_{j+2}^t$

represent the vacant space at the site $j+1$ and $j+2$, respectively. Moreover, let us define the maximum number of cars at site j that can move is defined by $b_j^t \equiv \min(U_j^t, L - U_{j+1}^t)$. Then cars that move only one site forward is given by $\min(b_j^t - a_j^t, L - U_{j+1}^t - a_{j-1}^t)$, where $L - U_{j+1}^t - a_{j-1}^t$ represents vacant space after all the cars moving two sites have moved. All sites are updated synchronously under this rule. Therefore, considering the number of cars entering into and escaping from site j, evolutional rule of EBCA is given by

$$\begin{aligned} U_j^{t+1} &= U_j^t + a_{j-2}^t - a_j^t \\ &\quad + \min(b_{j-1}^t - a_{j-1}^t, L - U_j^t - a_{j-2}^t) - \min(b_j^t - a_j^t, L - U_{j+1}^t - a_{j-1}^t) \\ &= U_j^t + \min(b_{j-1}^t + a_{j-2}^t, L - U_j^t + a_{j-1}^t) - \min(b_j^t + a_{j-1}^t, L - U_{j+1}^t + a_j^t). \quad (4) \end{aligned}$$

It is noted that (4) includes the model of Fukui and Ishibashi[12] as a special case if we take $L = 1$. In this paper we do not consider the flow limiter M in new model (4) for the sake of simplicity.

Let us analyze the traffic flow described by (4). The flow in this case is defined by

$$q^t \equiv \frac{1}{KL} \sum_{j=1}^{K} \min(b_{j-1}^t + a_{j-2}^t, L - U_j^t + a_{j-1}^t). \quad (5)$$

In the followings we restrict ourselves to the case $L = 2$. The fundamental diagram for this rule is given in Fig.4. If we choose all the possible combinations of 0,1 and 2 as initial conditions, we obtain a diagram shown in Fig.4(a). Fig.4(b) also shows the fundamental diagram of (4), but it is drawn by a finite number of random initial conditions. In both cases, we can see discontinuity around the transition region. The steady state line shows no longer a hat shape but "inverse λ" shape, and this shape is similar to that of real traffic flow given in Fig.1 if we average fluctuations. In Fig.4(a), we see that there are two steady states, i.e., free and congested state, in the transition region $1/3 \leq \rho \leq 1/2$. In Fig.4(b), the free flow line becomes shorter compared with that of Fig.4(a). These indicate that the states of high flow are highly ordered and therefore can not be reached starting from random initial conditions. Such states of high flow, although they are rarely observed in a real traffic

flow, are important in considering the transition from free to congested flow[16][17]. It is an advance of our model that we can prepare special initial configurations for generating high flow, and behaviors of them will be discussed in the next section.

It should be noted that evolution of the flow can show damping oscillation(Fig.5) in the course of time starting from random initial conditions in the region $1/3 \leq \rho \leq 1/2$, although it monotonously increases outside this region. In BCA case, it is proved that the flow monotonously increases at any ρ[18]. We will discuss why this oscillation occurs in EBCA in the next section.

Let us explain why the multiple states appear when higher velocity is introduced. Fig.6 shows a schematic diagram of Fig.4(a). The dotted line $O - A - B$ represents the fundamental diagram of BCA which is given in Fig.2. As mentioned above, two kinds of steady states are degenerated on the line in the case of BCA with $L = 2$. For example, in BCA two states are degenerated on the point A: $\cdots 111111111 \cdots$ and $\cdots 2020202020 \cdots$ if K is even. When we consider the higher velocity, these states separate into D and A respectively in Fig.6. This is because the state $\cdots 2020202020 \cdots$ cannot increase its velocity due to the full-packed sites "2", although the state $\cdots 111111111 \cdots$ can do. Similarly, it is apparent that states consisted of "0" and "1", which are on line $O - A$ in BCA, will shift to line $O - D$ in EBCA. Therefore, the slope of $O - D$ is 2, while that of $O - A$ in BCA is 1, and these slopes represent the maximum speed of each model.

Next, we consider states consisted of "0" and "2". These are on the hat $O - A - B$ in BCA, and on the hat $O - C - B$ in EBCA. We see that the peak of the triangle is shifted from $\rho = 1/2$ to $\rho = 1/3$. The shift of the peak to the lower density is already obtained by Fukui and Ishibashi[12]. The reason is as follows: if states of "0" and "2" is $\rho \leq 1/3$, then there are two vacant spaces in average in front of "2". Thus cars can increase its velocity from 1 to 2. When ρ exceeds 1/3, we cannot increase its velocity due to the full-packed sites.

Numerical experiments also show that steady states of "1" and "2" in BCA does not

increase its flow when the higher velocity is introduced. This is also because there are enough site "2" that blocks the traffic flow. Then the line $A-B$ does not change in EBCA. Taking these facts into consideration, the multiple states will appear between $1/3 \leq \rho \leq 1/2$ when higher velocity is introduced due to the separation of degenerated states.

4 Unstable free flow and shock wave

Let us consider in detail about the new branch $C-D$ in Fig.6. We can observe that the steady state near D in $C-D$ is unstable with respect to 'perturbation'. We give a perturbation to a state by shifting a car to an appropriate vacant space. Let us consider a perturbation from the state $\cdots 11 \cdots$ to the state $\cdots 20 \cdots$. Physically, this means that there are at least two successive sites of 1, and the front car decreases its speed and consequently the site behind it becomes fully-packed site "2". This perturbation apparently does not change the average car density. Then time evolution of the state $\cdots 1111111111 \cdots$ on D with respect to the perturbation is shown in Fig.7. We can prove that the state D transits to congested state A after enough time(Fig.8). From Fig.7, the tail of the string $22 \cdots 2$ expands to backward as fast as "0" at the front advances, and the front of the string $22 \cdots 2$ expands to backward with half speed of them. Therefore at sufficiently large t, we see that the number of "2" $\sim n$ and the number of "1" $\sim 3n \times 2/3 = 2n$. Considering that the car at site "2" cannot move and the car at the site "1" can move 2 site ahead per time, the mean velocity from the tail of the string $22 \cdots 2$ to the front of "0" is

$$< V > \sim \frac{2n \times 2}{2 \times n + 2n} \sim 1. \tag{6}$$

Of course the average car density keeps $\rho = 1/2$ during the time evolution, and periodic boundary condition does not change the above discussions. Thus the traffic flow $q = \rho < V >$ will eventually approach to $1/2$.

Numerical experiments show that state on line $C-D$ transits to $C-A$ under an ap-

propriate perturbation. This fact means that states of free traffic flow are unstable against perturbation if car density is high ($1/3 < \rho$). If only one car decreases its speed in this unstable state of free phase, then whole traffic flow will eventually become into the congested phase. The existence of the unstable branch is also discussed in [21] in relation to the model of modified version of Nagel and Schreckenberg and our results have good agreement with their discussions.

Moreover, it is interesting to note that a state near C on $C-A$ can transit to $C-D$ under an appropriate perturbation as shown in Fig.8. For example, let us consider the steady state 110110111110 with period $K = 12$ is on $C - D$. If we we perturb it to 110110120110, it becomes a steady state on $C - A$. It is clear that if we perturb the latter state to the former, we also obtain a transition from $C - A$ to $C - D$. In this case the effect of the perturbation does not expand to the whole state. However, about a state near A on $C-A$, it can not transit to $C - D$ under a perturbation since fully-packed sites are too many. Therefore the stability of the new branch $C - D$ is summarized as follows: states near D on $C - D$ are unstable and those near C on $C - D$ are stable under perturbation.

The stability of new branch $C - D$ have an important role on the time evolution of the flow. As we see in Fig.5, the flow can show a damping oscillation in the transition region $1/3 \leq \rho \leq 1/2$. If we start from a state near D on $C - D$ with some perturbation, then fully-packed sites will grow backward and the flow will decrease in the course of time. As we impose periodic boundary condition in this paper, the growth of congested sites will stop and new steady flow will appear after a while. In the formation of the new steady flow, it is sometimes observed that jam is partially cleared. Therefore the damping oscillation of the flow is seen in the transition region.

Finally let us consider a situation that a congested state exists in a free flow. It can be inferred that boundaries which separate the congested and the free state will move like a shock wave. To make discussions easier, let us consider an infinite space site in place of a periodic one. There exists a steady congested state $\cdots 121212 \cdots$ which gives a point P and

a free state $\cdots 010101 \cdots$ which gives a point Q in Fig.8. Let us consider an initial state where a part of the former exists in the background of the latter as shown in Fig.9(a). From the time evolution of this state, we can see that the shock wave which separates the left free region and the tail of the congested region propagates backward with the velocity calculated by the slope of the line $Q - P$ in Fig.8. This is proved by considering the conservation of number of cars. The conservation law of the number of cars at a boundary between free and congested regions is given by $\rho_f(v_f + c) = \rho_j(v_j + c)$, where $\rho_f(\rho_j)$ and $v_f(v_j)$ is density and velocity of the state $Q(P)$ and c is a velocity of the boundary, i.e., the shock wave. Since flow q is defined by $q = \rho v$, we obtain $c = (\rho_f v_f - \rho_j v_j)/(\rho_j - \rho_f) = (q_f - q_j)/(\rho_j - \rho_f)$, which is the slope of the line $Q - P$. This holds any states between $O - C$ and $C - B$ and the velocity is less than -1. Also, the state of the head of P become the state indicated by C, and the slope $C - P$ is -1. Thus the congested state P vanishes after a time due to the difference of the velocity of both boundaries of P.

Next, we consider an unstable free state $\cdots 01111011110 \cdots$ giving R in Fig.8. Let us make an initial state by putting a part of $\cdots 121212 \cdots$ giving P in the background of $\cdots 01111011110 \cdots$ as shown in Fig.9(b). In this case, the new point is that the tail of $\cdots 121212 \cdots$ region shows stagnation of car flow and the stagnation region corresponds to the state $22 \cdots 22$ giving B in Fig.8. Moreover, the stagnation region grows wider to the opposite direction in the course of time. This is interpreted as follows. The unstable free flow can be considered as a state of overloading of cars. Then it is easily stagnated due to perturbations as shown above. The boundary between regions of R and B propagates backward with the velocity calculated by the slope of line $R - B$ and the boundary between regions of B and P moves with the velocity of the slope of line $B - P$, i.e.,-1. Therefore the difference of the velocity of both boundaries of B will make the stagnated region wider.

It is noted that in both cases, we see that the head of region of P becomes the region indicated by C in Fig.8. This shows that cars do not increase their velocity to the maximum speed in the unstable region when they get out of the congested region.

5 Conclusion

We propose a new deterministic CA model of traffic flow in this paper, EBCA, which shows multiple states in the fundamental diagram. The model can be considered as the multi-value and higher-velocity generalization of the rule–184 CA. A new point is that the free moving state and the congested state coexist at $1/3 \leq \rho \leq 1/2$ in the fundamental diagram in the case $L = 2$, while in the case of $L = 1$ multiple states do not exist[12]. It is shown that the states in the new branch $C - D$ transits to $C - A$ under perturbation in Fig.8. The perturbation considered in Sec.4 corresponds to a kind of braking. Since in NS model, braking probability is introduced as noise, then the unstable part of the new branch may disappear by introducing noise in EBCA. Introducing the influence of noise will make our model more realistic.

We give the following remarks. Since our model is deterministic, analytical methods such as the ultradiscrete method[19] can be applied to study the multiple states in detail. Moreover, if we consider the general L and general V of BCA, other multiple states will appear in the diagram in the case $L \geq 2$, and introducing the flow limiter M in the EBCA suppresses the multiple states. Detailed analysis on these facts, on density fluctuations due to noise or open boundaries, and on comparison with other traffic flow models with metastable states will appear in succeeding papers.

Acknowledgment

The authors are grateful to Professor Hisao Hayakawa for fruitful discussions and helpful comments. This work is partially supported by Grant-in-Aid from the Ministry of Education, Science and Culture (No.9750078, 9750087).

References

[1] H. Greenberg, Oper. Res., **7** (1959) pp.79.

[2] B. S. Kerner and P. Konhäuser, Phys. Rev. E, **48** (1993) p.2335.

[3] G. F. Newell, Oper. Res., **9** (1961) p.209.

[4] M. Bando, K. Hasebe, A. Nakayama, A. Shibata and Y. Sugiyama, Phys. Rev. E. **51** (1995) p.1035.

[5] M. Bando, K. Hasebe, K. Nakanishi, A. Nakayama, A. Shibata and Y. Sugiyama, J. Phys. I France. **5** (1995) p.1389.

[6] Traffic Engineering (in Japanese), T. Sasaki and Y. Iida, Eds. (Kokumin Kagakusha, 1992).

[7] L. C. Edie, Oper. Res., **9** (1961) p.66.

[8] F. Navin and F.Hall, ITE Journal, August, (1989) p.31.

[9] S. Wolfram, *Theory and Applications of Cellular Automata* (World Scientific, Singapore, 1986).

[10] K. Nagel and M. Schreckenberg, J. Phys. I France **2** (1992) p.2221.

[11] M. Schreckenberg, A. Schadschneider, K. Nagel, N. Ito, Phys. Rev. E. **51** (1995) p.2939.

[12] M. Fukui and Y. Ishibashi, J. Phys. Soc. Jpn., **65** (1996) p.1868.

[13] H. Fukś and N. Boccara, to appear in Int. J. Mod. Phys. C.

[14] B. Eisenblätter, L. Santen, A. Schadschneider and M. Schreckenberg, Phys. Rev. E **57** (1998) p.1309.

[15] M. Takayasu and H. Takayasu, Fractals **1** (1993) p.860.

[16] A. Schadschneider and M. Schreckenberg, Ann. Physik **6** (1997) p.541.

[17] R. Barlovic, L. Santen, A. Schadschneider and M. Schreckenberg, cond-mat/9804170.

[18] K. Nishinari and D. Takahashi, J. Phys. A **31** (1998) p.5439.

[19] T. Tokihiro, D. Takahashi, J. Matsukidaira and J. Satsuma, Phys. Rev. Lett. **76** (1996) p.3247.

[20] S. Yukawa, M. Kikuchi and S. Tadaki, J. Phys. Soc. Jpn., **63** (1994) p.3609.

[21] M. Paczuski and K. Nagel, *Workshop in Traffic and Granular Flow*, p.73, edited by D. E. Wolf, M. Schreckenberg and A. Bachem, (World Scientific, Singapore, 1996).

Figure Captions

Fig.1 The observed data of flow (vehicles/5min.) versus occupancy of the road. This diagram was taken by Japan Highway Public Corporation.

Fig.2 The fundamental diagram in the case $L = 2$ of BCA. The number of samples is 1000 and the system size used for the simulation is $K = 50$.

Fig.3 The fundamental diagram in the case $L = 3$ and $M = 1$ of BCA. The number of samples is 1000 and $K = 50$.

Fig.4 The fundamental diagram of EBCA. We set $K = 50$ and initial conditions are given by (a)all the possible combinations of 0, 1 and 2 (b)random states of 1000 samples.

Fig.5 Typical time evolution of the flow of EBCA in the region $1/3 \leq \rho \leq 1/2$. The system size is $K = 50$.

Fig.6 The schematic diagram of Fig.1 and Fig.4(a). The hat OAB represents the fundamental diagram of BCA and the lines OD and CB represents that of EBCA.

Fig.7 Time evolution of $\cdots 11120111 \cdots$ by EBCA.

Fig.8 The schematic diagram of Fig.4(a). States on the line $C - D$ can transit to those on the line $C - A$ under some perturbations.

Fig.9 (a)Time evolution of free stable region containing congested region. The shock wave propagates backward and the region ahead the congested one becomes the state giving C in Fig.8.

(b)Time evolution of unstable free region containing congested region. The stagnation of car flow occurs behind the congested region. White, gray and black square denote a site with value 0,1 and 2, respectively.

Fig.1

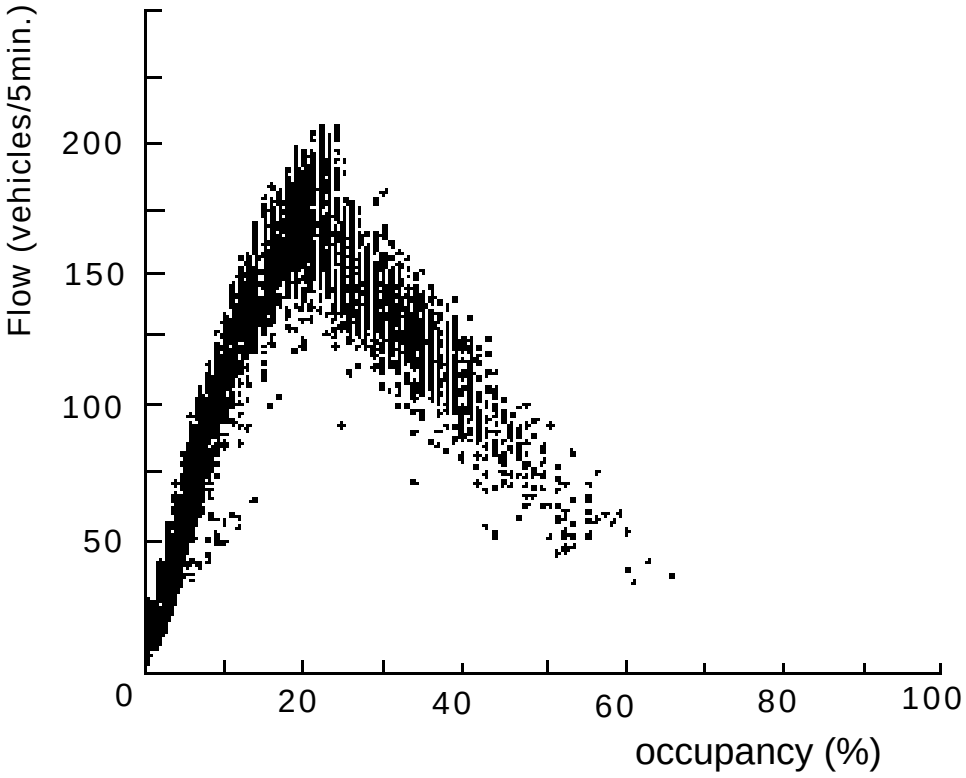

Fig.2

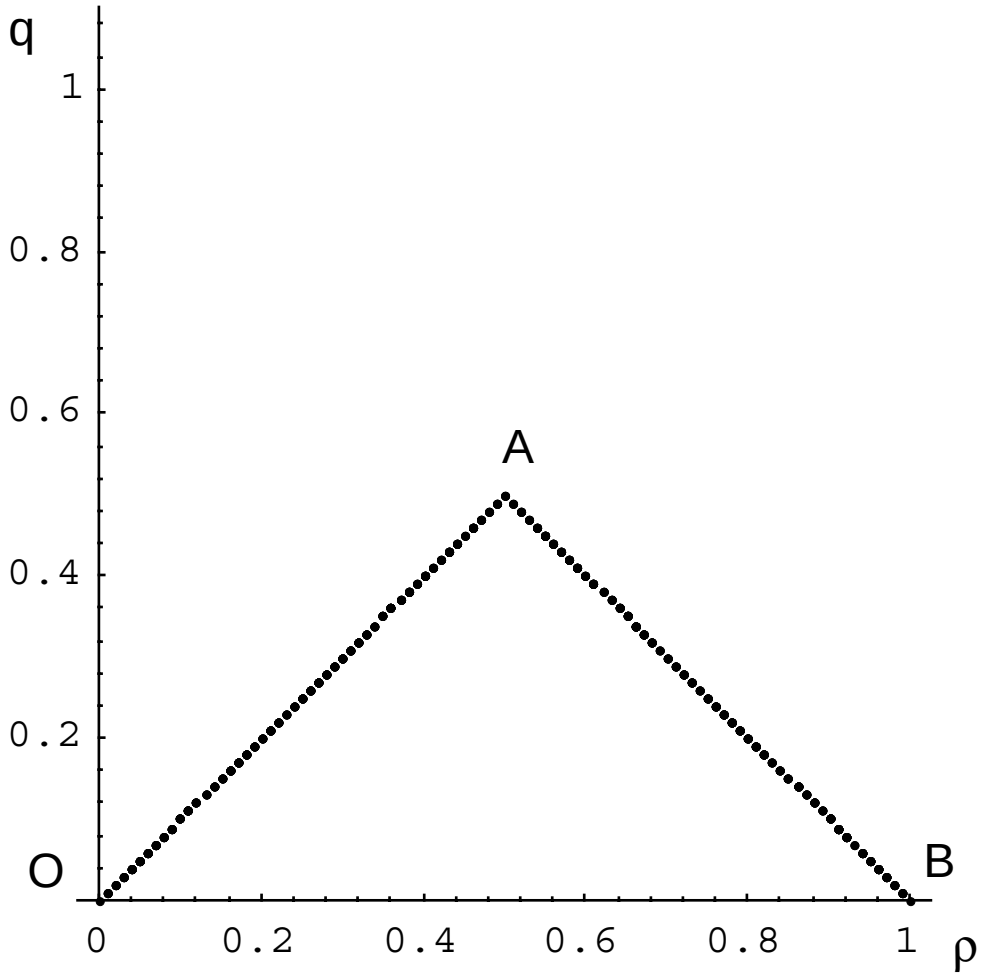

Fig.3

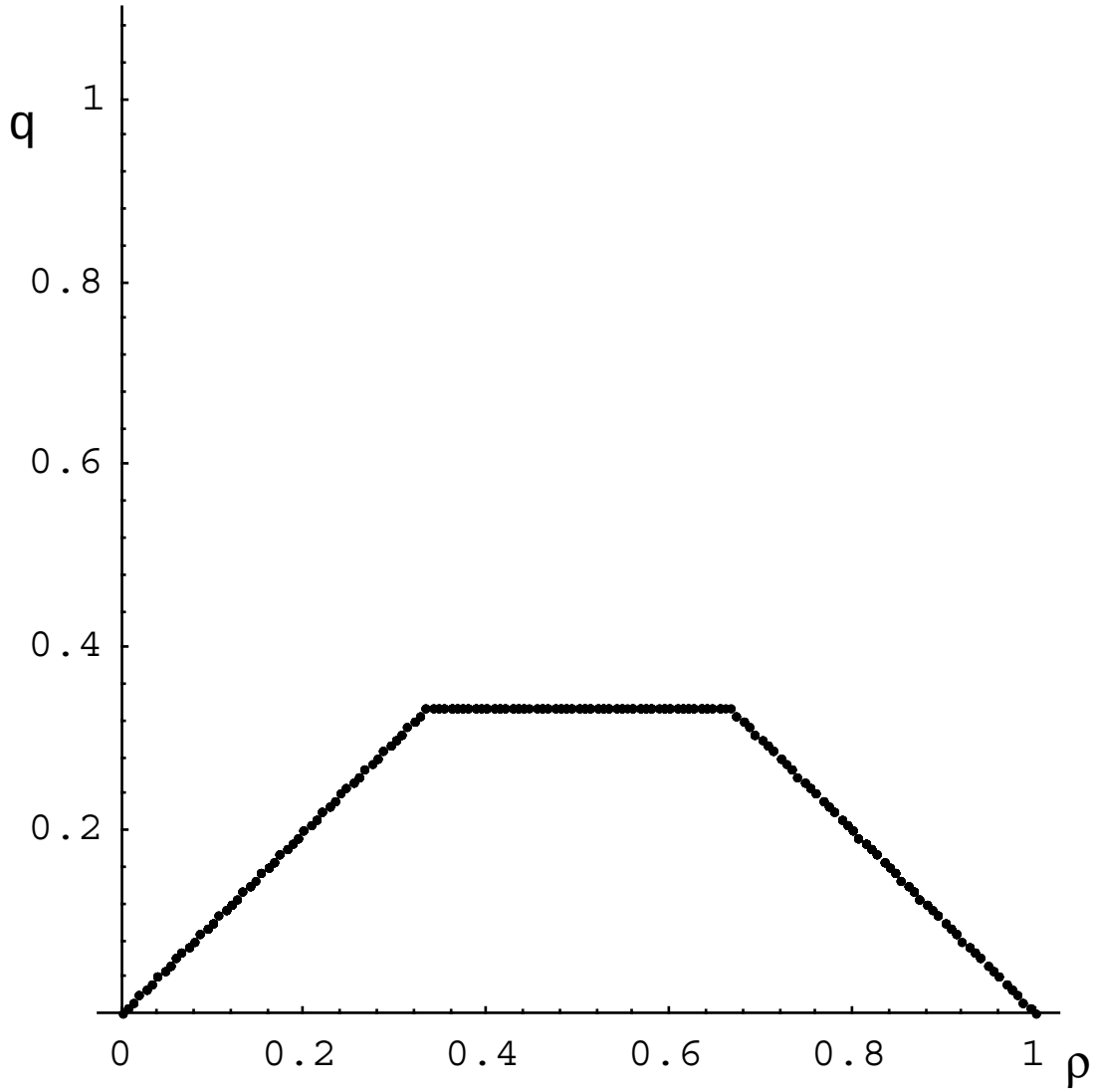

Fig.4(a)

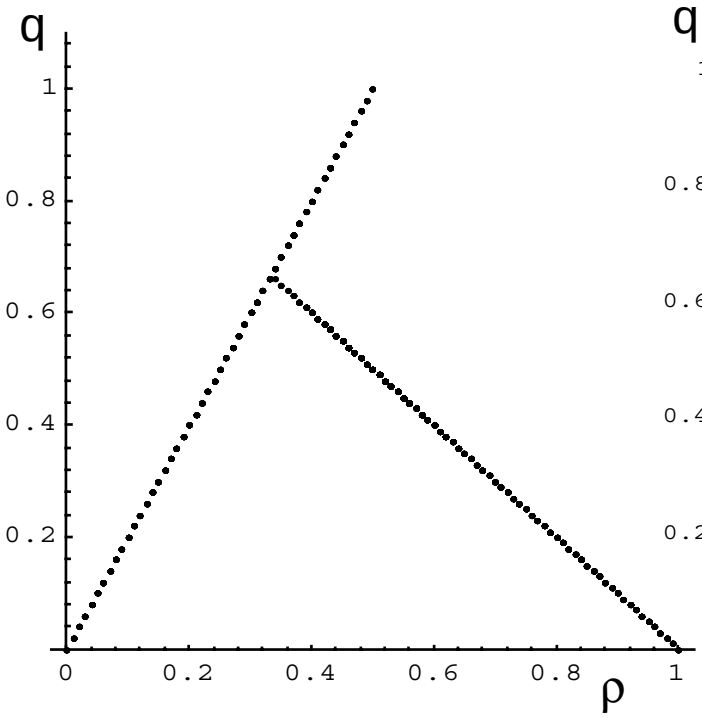

Fig.4(b)

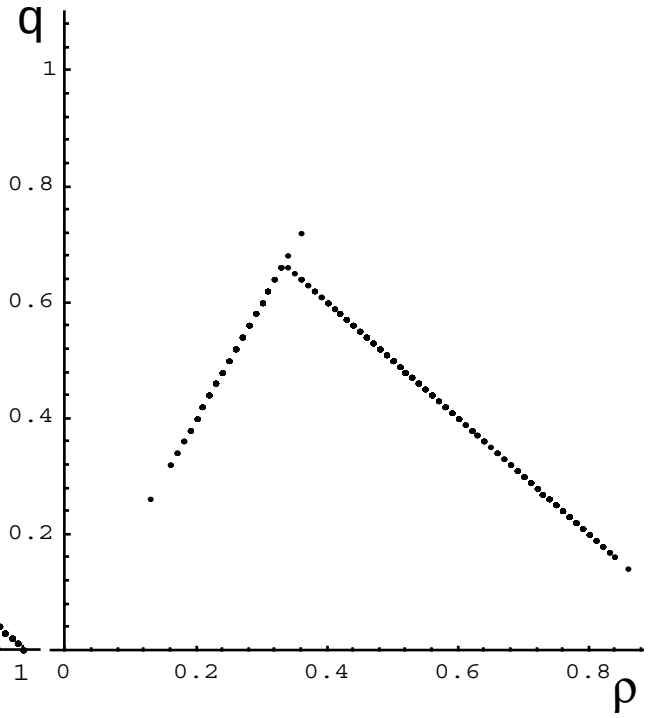

Fig.5

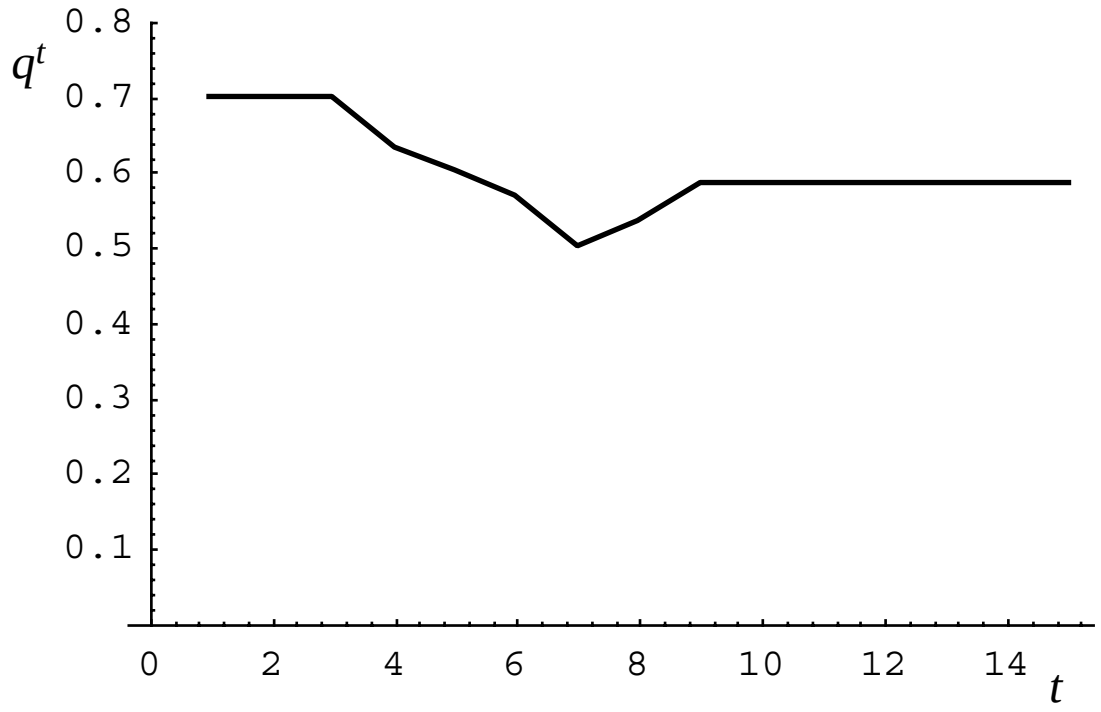

Fig.6

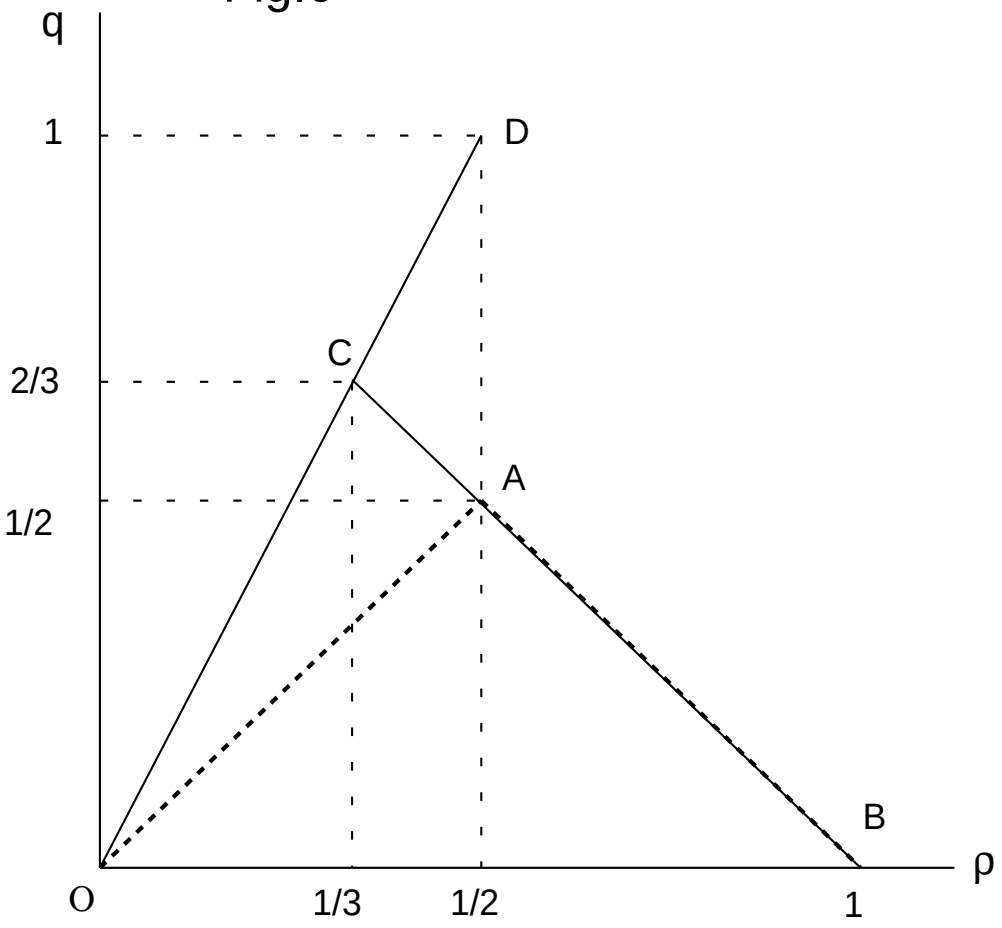

Fig.7

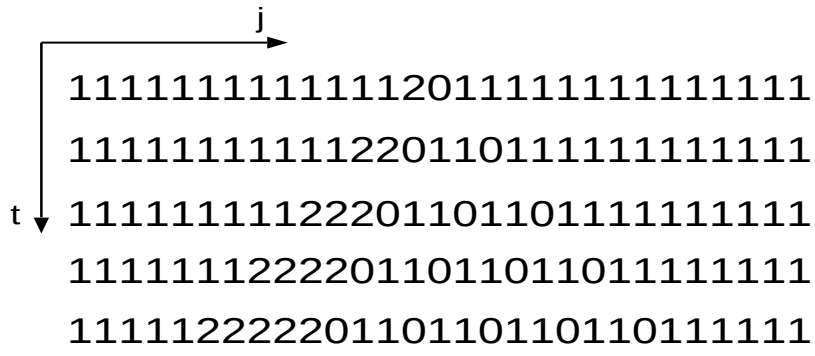
j
t
11111111111112011111111111111
11111111111220110111111111111
11111111122201101101111111111
11111112222011011011011111111
11111222220110110110110111111

Fig.8

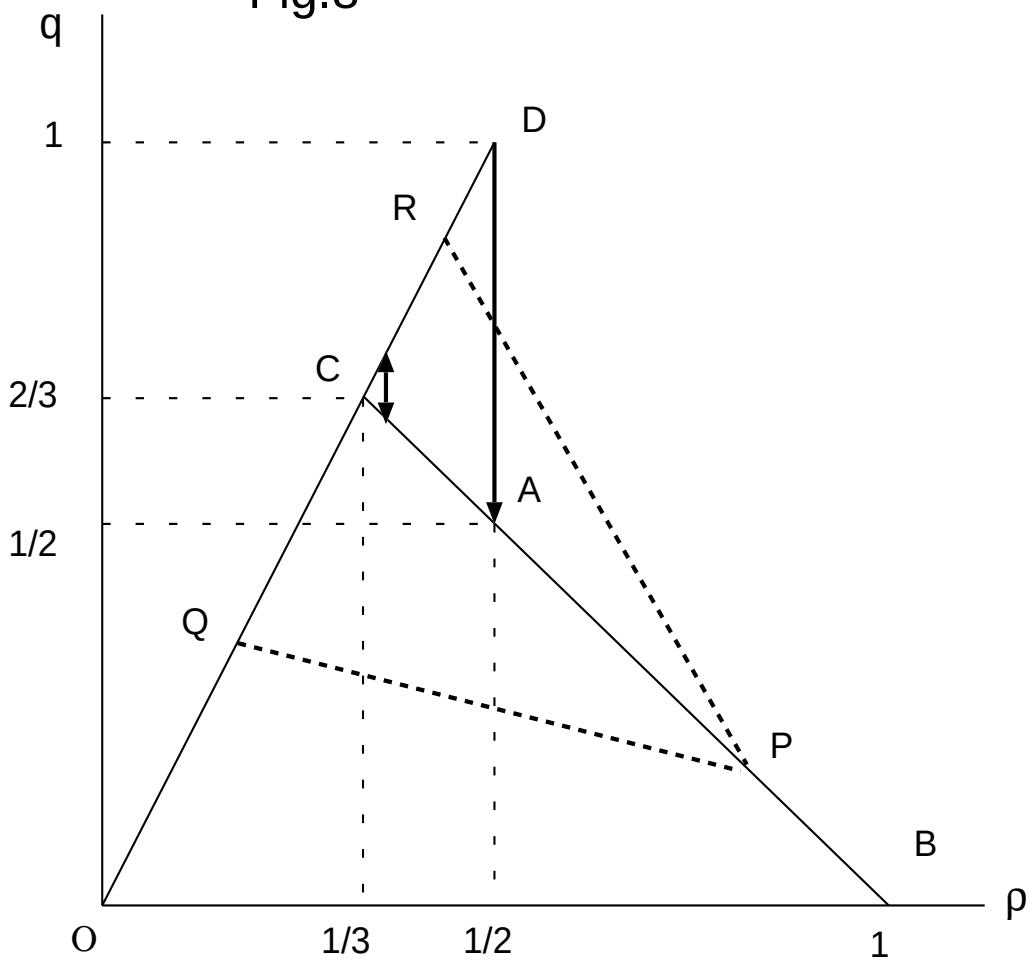

Fig.9(a)

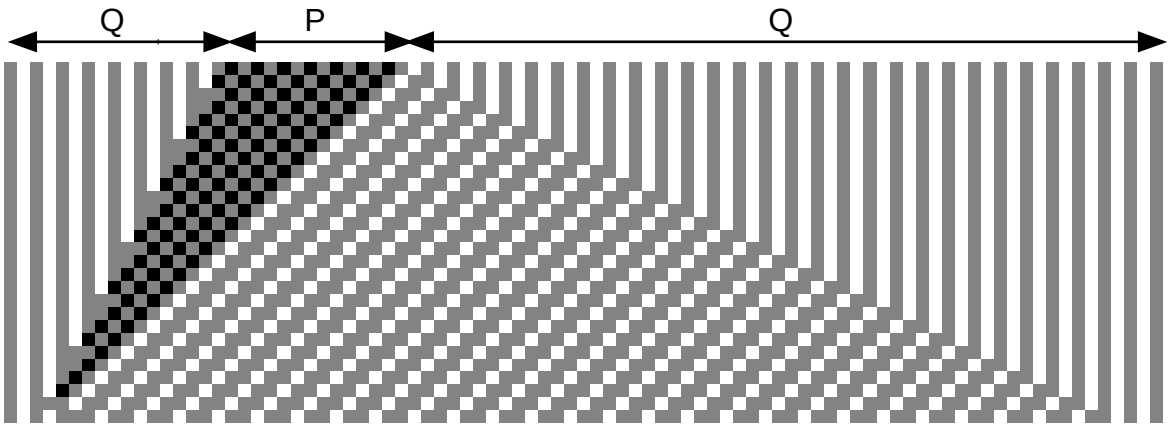

Fig.9(b)